Available online at www.sciencedirect.com
ScienceDirect
Sedimentary Geology 195 (2007) 113–134
Sedimentary Geology
www.elsevier.com/locate/sedgeo

Oxfordian ramp system (La Manga Formation) in the Bardas Blancas area (Mendoza Province) Neuquén Basin, Argentina: Facies and depositional sequences

Ricardo M. Palma [a,*], José López-Gómez [b], Ricardo D. Piethé [c]

[a] *Departamento de Ciencias Geológicas, Facultad de Ciencias Exactas y Naturales, Universidad de Buenos Aires-CONICET, Pabellón II. 1428 Buenos Aires, Argentina*
[b] *Instituto de Geología Económica, CSIC-UCM, Facultad de Geología, Universidad Complutense, Antonio Nováis 2, 28040 Madrid, Spain*
[c] *Departamento de Ciencias Geológicas, Facultad de Ciencias Exactas y Naturales, Universidad de Buenos Aires, Pabellón II. 1428 Buenos Aires, Argentina*

Received 12 December 2005; received in revised form 28 June 2006; accepted 5 July 2006

Abstract

The outcrops of the Oxfordian La Manga Formation at Bardas Blancas, Neuquén Basin, west-central Argentina, allow the recognition of six different depositional facies (A to F) on the basis of sedimentological analysis, taphonomic attributes and microfacies studies. These depositional facies correspond to outer ramp (A), middle ramp (B), inner ramp— oolitic shoal (C), inner ramp margin (patch reef) (D), lagoon deposits (E), and a paleokarst surface (F). Outer ramp deposits which are not completely represented, consist of greyish carbonate beds, where the fabric of the shell beds (gryphaeids) reflects the action of waves and currents. Middle ramp deposits consist of a packstone–grainstone lithofacies indicating the importance of storm processes and is dominated by ooids, intraclasts, pelecypods, echinoderms and gastropods which accumulated on a middle-ramp storm-dominated shoreface. Trace fossils belong to the *Skolithos* and *Cruziana* Ichnofacies characterizing the upper, lower and middle shoreface setting respectively. The inner ramp deposits consist of oolitic grainstones and subordinate packstones shoal with a small sponge bioherm at the base. Different types of ooids, peloids and coated grains are abundant, as well as skeletal fragments of molluscs, echinoderms and corals. Lithofacies and microfacies studies suggest a high energy and shallow-water depositional setting. The inner ramp margin deposits consist of reef core facies, fore and back reef facies characterized by a scleractinian community of relatively low generic diversity. The rich associated fauna consists of bivalves, echinoids, serpulids, bryozoans, dasycladacean algae and cyanophytes, as well as foraminifers and ostracods. The growth forms of the corals are indicative of shallow well illuminated water. Both the back and fore reef deposits suggest intensive reworking by storm waves or currents. The lagoon deposits consist of bioclastic and peloidal wackestones as well as bioclastic–intraclastic packstones which accumulated on a lagoon under intermittently agitated water in a shallow subtidal to intertidal settings. A stratiform breccia with both matrix and clasts supported fabrics is interpreted as paleokarst. The clasts are derived from the rocks of oolitic shoal and inner ramp margin (patch reef).

The six depositional facies are included into a major organizational framework of three third-order depositional sequences (DS-1, DS-2, DS-3) mainly represented by transgressive and highstand systems tracts stages with sequence boundaries of regional importance. The general depositional evolution is here related to the slow subsidence experienced during the Oxfordian–earliest

* Corresponding author.
E-mail address: palma@gl.fcen.uba.ar (R.M. Palma).

0037-0738/$ - see front matter
doi:10.1016/j.sedgeo.2006.07.001

Kimmeridgian time related to tectonic inversion in the Neuquén Basin. A four step (architectural and sedimentary) schematic model of the response of the platform to sea-level changes is proposed.

Keywords: Jurassic; La Manga Formation; Oxfordian; Neuquén Basin; Facies; Depositional sequence

1. Introduction

The Neuquén Basin is developed at the west margin of South American platform and limited by a magmatic arc to the west and a tectonic foreland to the east. The foreland consisted of the Sierra Pintada belt to the northeast and the North Patagonia massif to the south. The Neuquén Basin is a typical retro-arc foreland basin that developed to the east of the main Cordillera between 36°S and 39°S. The most important papers describing the geologic setting of the region include those of Digregorio and Uliana (1980), Groeber (1946), Gulisano et al. (1984), Mitchum and Uliana (1985), among others. Legarreta and Gulisano (1989) described four tectonic episodes of basin development: 1—rifting (Upper Triassic–Lower Jurassic), 2—thermal subsidence (Lower Jurassic–Upper Cretaceous), 3—subsidence due to loading (Upper Cretaceous–Early Tertiary) and 4—Andean tectonism (Early Tertiary–Early Quaternary).

The basement consists of Early Paleozoic to Late Triassic metamorphic, plutonic, volcanic and sedimentary rocks. Groeber (1946) identified three depositional cycles: *Jurásico*, *Ándico* and *Riográndico*. Legarreta and Gulisano (1989) agreed generally with the validity of the Groeber's cycles, and emphasized the importance of eustatic variations in the development of depositional sequences.

The Jurassic sequences are part of the lower supersequence of Legarreta and Gulisano (1989) and includes three mesosequences: Precuyo, Cuyo and Lotena. The Lotena Mesosequence consists of five depositional sequences that include marine and continental facies (Lotena Fm.), carbonate deposits (La Manga Fm.), and evaporites (Auquilco Fm.). The Lotena Mesosequence developed from Middle Callovian to Late Oxfordian–Kimmeridgian times.

Studies of the La Manga Fm. have been focussed mainly on their lithostratigraphy, biostratigraphy and paleontology (Groeber et al., 1953; Stipanicic, 1965, 1996; Leanza, 1981; Riccardi, 1984; Riccardi, 1992, amongs others) and its sedimentological interpretation (Legarreta, 1991; Lo Forte and Palma, 2002; Palma et al., 2003, 2004, 2005) as well as diagenetic aspects of the succession (Palma et al., 1997; Palma and Lo Forte, 1998), however, detailed sedimentological and paleogeographical work is still necessary.

This paper examines in detail the lithostratigraphy and sedimentology of La Manga Fm. (60 m) in the Bardas Blancas area (Fig. 1) and provides sequence stratigraphy and paleoenvironmental interpretations of the sedimentary succession. On the basis of lithology, sedimentary structures, taphonomic attributes and microfacies, the strata of La Manga Fm. have been organized into different lithofacies that constitute six depositional facies (A to F) representing outer carbonate ramp, middle ramp, inner ramp margin (patch reef), inner ramp represented by oolitic shoal and lagoonal deposits, and a paleokarst. The ages of the sediments are taken from Legarreta (1991) who based his analysis on data from ammonites described by Stipanicic (1951, 1965, 1969), Westermann (1967), Dellapé et al. (1979), Westermann and Riccardi (1984), and Riccardi (1984).

2. Geological setting

The Bardas Blancas area, located north of Neuquén Basin, Mendoza Province, forms a general folded terrain in which a very complete Jurassic sedimentary succession crops out above Upper Triassic volcanic rocks. This area is part of the so-called central Aconcagüa–Neuquén depocenter (Riccardi, 1983) which expanded to more than 100 km in neighbouring Chile.

During most of the Jurassic and the Cretaceous periods, the western side of this area of South America was part of a continental margin evolving under active convergence. The study area was part of the back-arc depocenter, in the east of the convergence margin and which was controlled by Mesozoic crustal stretching that did not lead to the development of oceanic crust. Regional (thermal sag style) subsidence controlled the Pliensbachian–Neocomian period in the basin and also the deposition of the Cuyo, Lotena and Mendoza Groups. This subsidence also included various inversion and fault-controlled stages (Vergani et al., 1995).

La Manga Fm. belongs to the Lotena Group (Callovian–Oxfordian) which corresponds approximately to the so-called Araucarian inversion bounded by two important unconformities (Fig. 2). Hiatuses and erosive surfaces separate the formations of the Lotena

Group, eastward of the study area, from the Potimalal area to the Bardas Blancas area; some units pinch out or become thinner and only those formations related to dominant transgressive pulses persist. La Manga Formation rocks which constitute most of the sedimentary record of this period of time in this area, show various

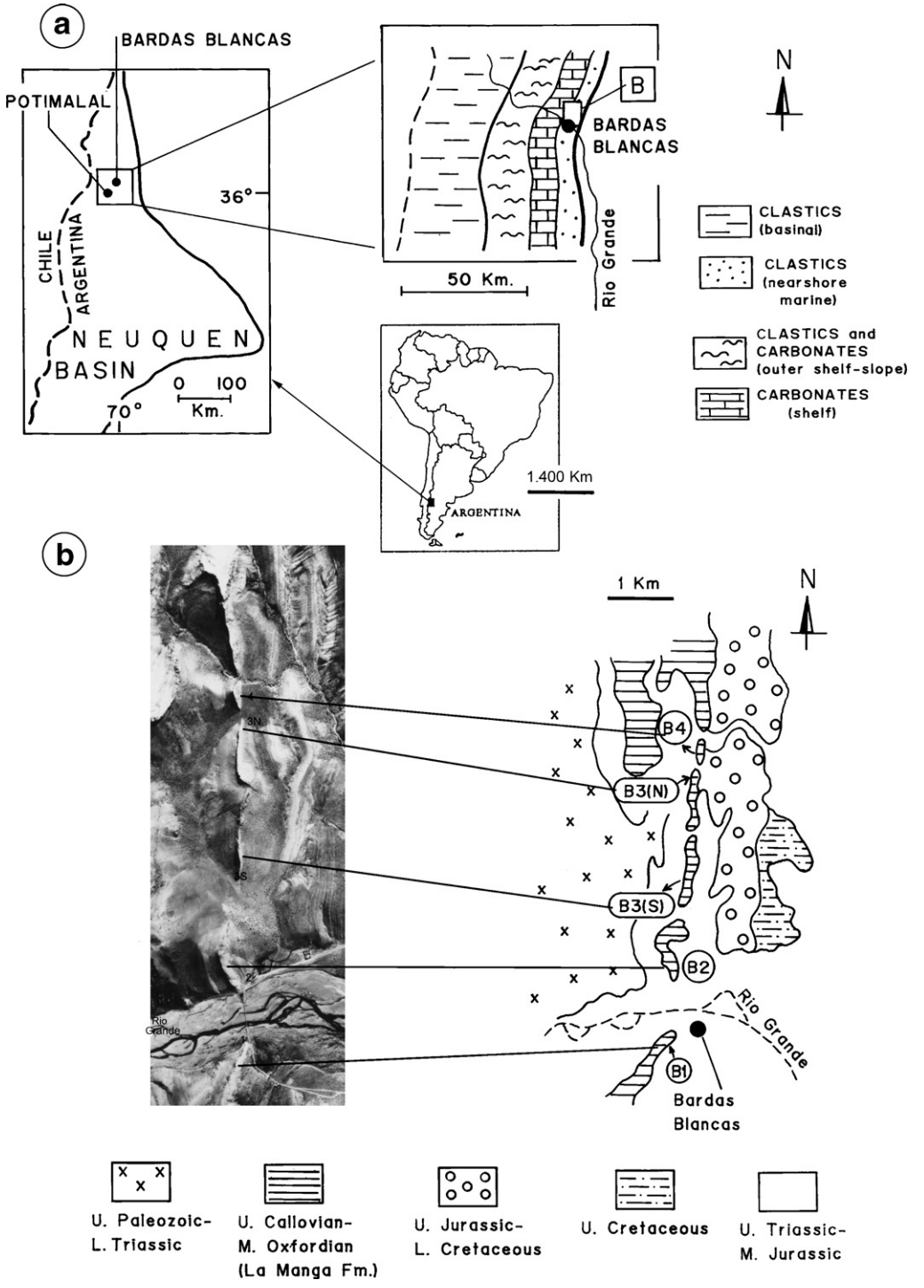

Fig. 1. Geographical and geological setting of the study area. a—mapping, modified from Legarreta (1991), represents main Callovian–Oxfordian units. b—aerial photograph schematic interpretation of the studied area. B1 to B4 (*Barda*-1 to *Barda*-4) represent the studied outcrops.

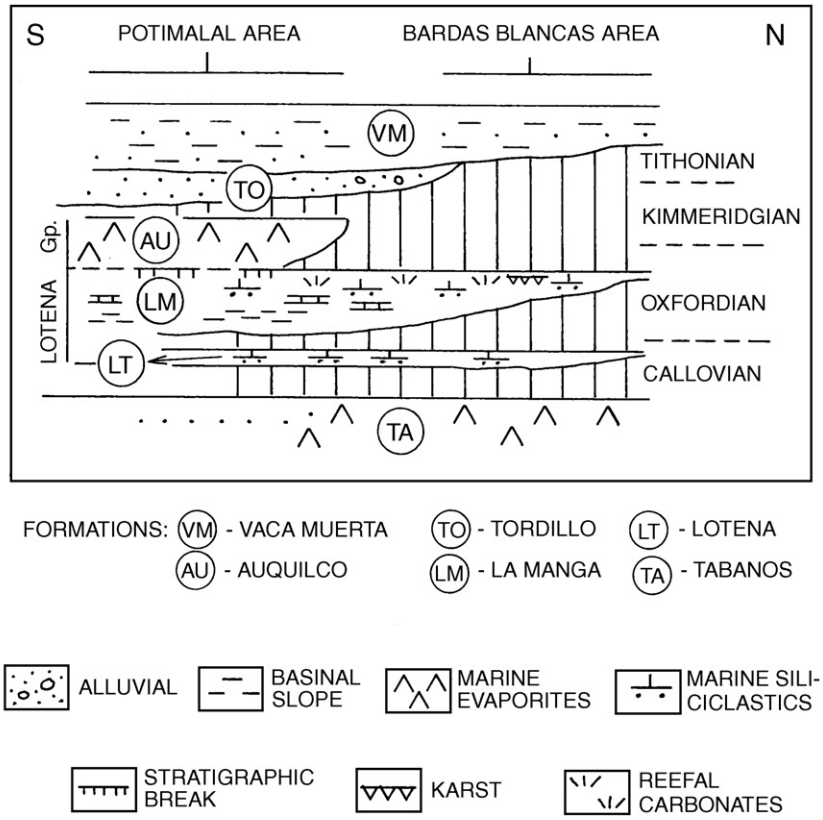

Fig. 2. Temporal and spatial range of the Callovian–Tithonian formations in the studied area. Figure not to scale.

transgressive cycles, and represents a clear craton-ward onlap resulting in a starved basin axis and depositional profiles lacking steep slopes as a result of rapid expansion on the broad depositional area of the earlier Callovian sediments (Legarreta, 1991). The persistence in position of this lithology in this area within 35–40°S latitude belt was the main factor which controlled the stratigraphic record (Legarreta and Uliana, 1996).

3. Depositional facies

This work is based on the detailed study of five complete sections in Bardas Blancas area: *Barda*-1, -2, -3 (S), -3(N) and -4 (Fig. 3). Each section is separated from the other nearest one by no more than 3 km and all of them occur along an approximately N–S lineament more or less parallel to the present-day Andean Cordillera.

Sediments description and interpretation are here presented from deep to shallow by means of six major depositional facies (A to F) which allow us a major organizational framework based on the Sequence Stratigraphy (Fig. 4). A brief description of each differentiated lithofacies is included in the text below and expanded sedimentological details are presented in Tables 1 and 2, and illustrated in Fig. 5, and the most frequently occurring microfacies types are illustrated in Fig. 6.

3.1. Greyish wackestone/packstone—outer ramp (A)

This is composed of greyish packstone–wackestone rich in well preserved molluscs shells (Fig. 5a), and rarely carbonate sandstones in the upper part. Beds are often massive or graded. The thickness ranges from 10 to 70 cm (mean of 30 cm). The lower contact is generally sharp and planar and occasionally erosive, whilst upper contact ranges from sharp to gradational. In thin section, four main categories of microfacies, based on the main grain types and relative proportion of allochemical components, were identified: Bioclastic packstones (MF-1), intraclastic–bioclastic packstones (MF-2), peloidal wackestones (MF-3) and bioclastic wackestones (MF-4), (Table 1), (Fig. 6a,b).

3.1.1. Interpretation

The presence of fragmented bioclastic material and subrounded intraclasts, together with the taphonomic

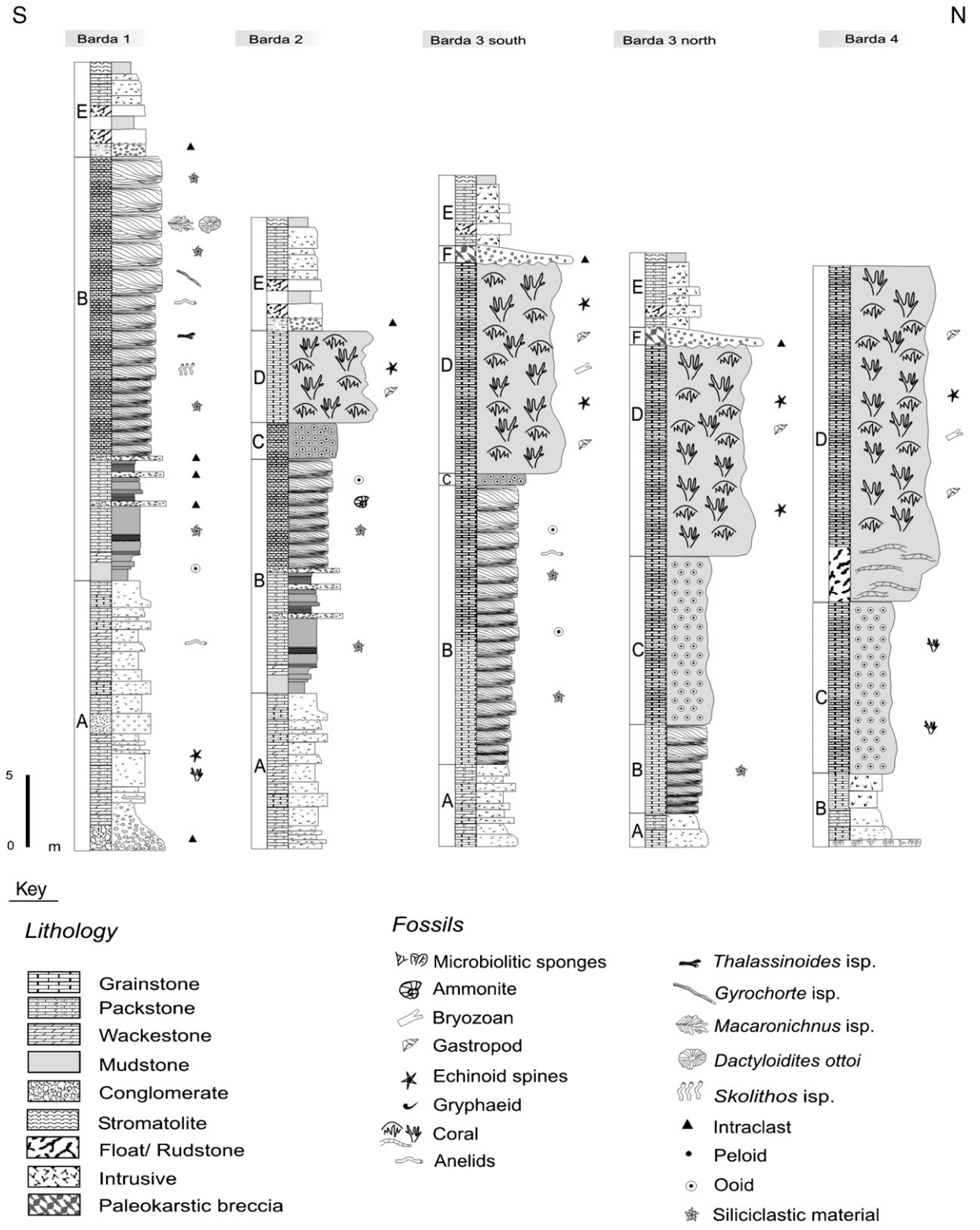

Fig. 3. General stratigraphic sections of the studied *Bardas*-1, -2, -3(S), -3(N) and -4. See Fig. 1 for their location.

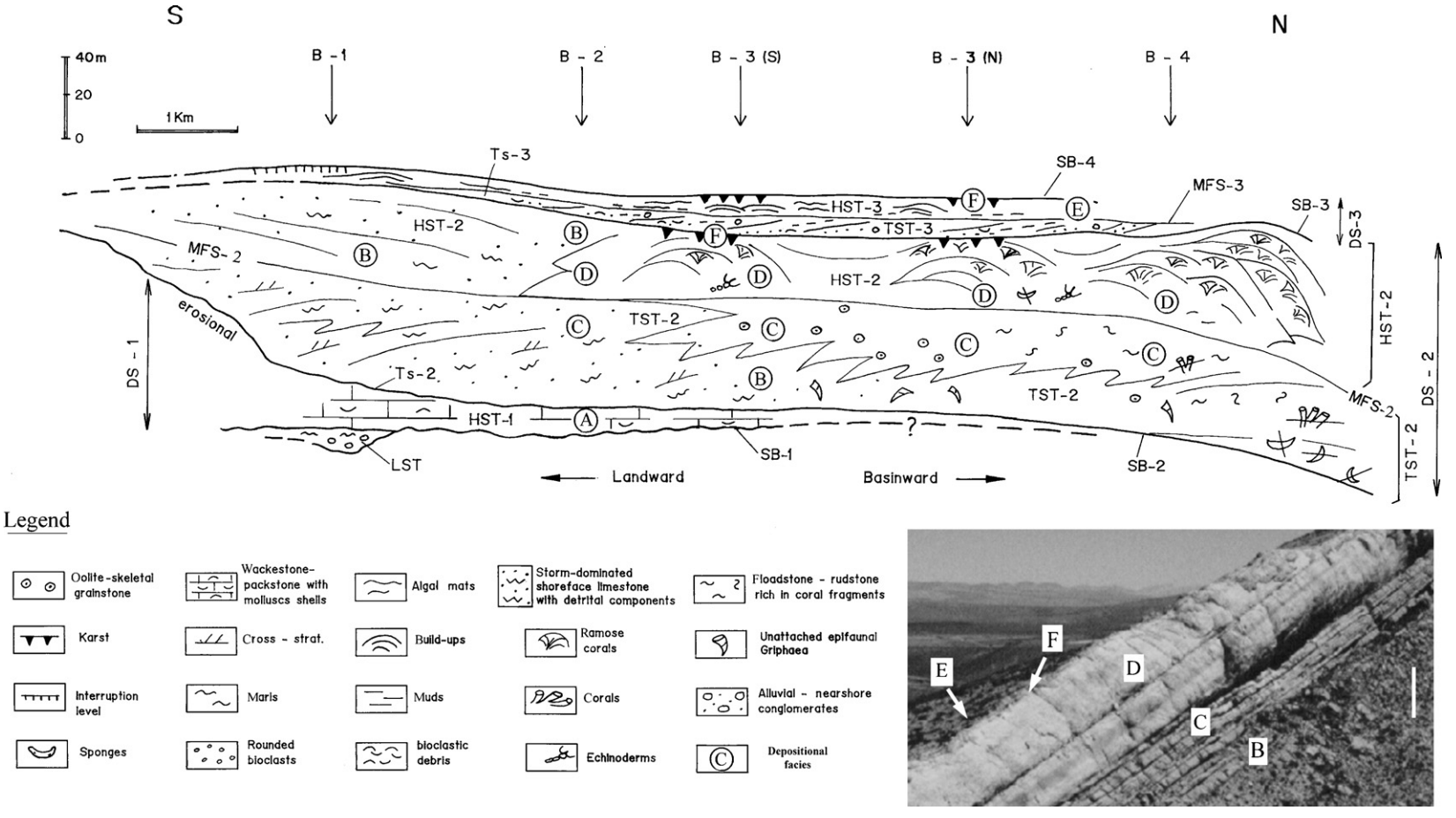

Fig. 4. Depositional sequences (DS-1, DS-2, DS-3), their systems tracts and differentiated depositional facies distribution in the studied area. B-1 to B-4 represent *Barda*-1 to *Barda*-4 (see Fig. 1 for their location). Capital letters (A to F) correspond with those used in the text. Picture represents a partial view of *Barda* 3(S) and its bar-scale is 5m. HST—highstand systems tract, TST—transgressive systems tract, SB—sequence boundary, DS—depositional sequence, MFS—maximum flooding surface, Ts—transgressive surface.

Table 1

Lithofacies	Important constituents	Sedimentary structures	Body and traces fossils	Taphonomy	Interpretation
Bioclastic packstones (MF-1)	Bioclasts peloids, ooids. Cavities filled by phreatic granular cement, and syntaxial cement	Medium- to thick, massive, graded, amalgamated	Bivalves, gastropods, echinoderms, serpulids, bryozoan	Disarticulated, fragmented, convex-up>>convex-down, random, nested fabrics, borings common, micritization. (Kidwell, 1991; Kidwell and Holland, 1991).	Storm deposits below fair-weather wave base. Outer ramp
Intraclastic–bioclastic packstones (MF-2)	Intraclasts, bioclasts, peloids, ooids	Medium- to thick, massive, graded	Bivalves, gastropods, echinoderms, serpulids, bryozoan, forams, calcispheres, oncoids, ooids	Disarticulated, more fragmented, convex-up>>convex-down, random, nested fabrics, borings common, micritization	Storm deposits below the fair-weather wave base. Outer ramp
Peloidal wackestones (MF-3)	Peloids, millimeters scales of undeterminated bivalves, peloidal matrix. Rims of blocky calcite cement	Fine- to medium bedded, massive, graded, and planar laminae, nodular stratification	Bivalves, forams, serpulids	Aragonitic forms preserved as molds. Micritization, convex-down, high articulation, microborings	Suspension in a low energy setting below the storm wave base. Firm ground development. Outer ramp
Bioclastic wackestones (F-4)	Peloids, millimeters scales of undeterminated bivalves. Peloidal matrix	Fine- to medium bedded, massive, graded, and planar laminae	Bivalves, Echinoderms, forams, bryozoan	Convex-down, micritization, microborings	Suspension in a low energy setting below the storm wave base. Outer ramp
Oopelbioclastic packstones	Ooids (types 1, 3, 5), peloids, bioclasts	Medium bedded, plane parallel laminae and graded lenses	Bivalves, Echinoderms, Forams, *Skolithos* isp.	Fragmentation, disarticulation	Upper shoreface. Middle ramp
Peloidal–bioclastic wackestones	Peloids, bioclasts, scattered ooids (type 3)	Medium-to fine bedded, wave ripple lamination	Bivalves, Echinoderms, *Dactiloidites otto Thalassinoides isp.*	Fragmentation, disarticulation	Lower shoreface. Middle ramp
Oolitic–peloidal Packstones–grainstones	Ooids (type 3, 5) peloids, bioclasts, quartz, feldspar, and lithic fragments	Medium- to fine bedded, graded and planar tabular cross-stratification. Alternate laminae of immature sandstones and oolitic–peloidal pack-grainstones	Bivalves, Echinoderms, *Skolithos* isp.	Fragmentation, disarticulation	Upper shoreface. Middle ramp
Peloointraclastic packstone–grainstones	Peloids, ooids (type 1, 3, 5) intraclasts, oncoids and siliciclastic particles	Medium- to fine bedded, massive	Bivalves, bioturbation	Fragmentation, disarticulation	Lower shoreface transition zone. Middle ramp
Oopelbio–grainstone–packstones	Ooids (type 1, 3, 5) peloids, bioclasts, oncoids	Medium- to fine bedded, swaley cross-stratification	Bivalves, echinoderms, oncoids, forams, *Acicularia* sp., *Heteroporella* sp., Cyanophytes, Skolithos *isp.*	Fragmentation, disarticulation, abrasion	Upper shoreface. Middle ramp
Oopelbiointra–grainstone–packstones	Ooids (type 1, 2, 3, 5) peloids, bioclasts, intraclasts, oncoids, and siliciclastic grains (up to 35%)	Medium- to thick bedded, hummocky cross-stratification, amalgamation	Bivalves, echinoderms, dasycladacean, cyanophytes, gastropods, serpulids, *Gyrochorte* isp., *Thalassinoides* isp., *Dactiloidites* ottoi *Macaronichnus* isp.	Fragmentation, disarticulation, abrasion	Lower-middle shoreface. Middle ramp
Calcirudites	Pebbles 3–8 cm from pack-grainstones	Medium bedded, massive	Bivalves	Fragmentation, disarticulation	Lower shoreface. Middle ramp
Siltstones	Quartz, feldspar, peloid	Very fine bedded, horizontal laminated	Extensive horizontal burrowing (fodidicnial)	Absent	Lower shoreface. Middle ramp

Table 2

Lithofacies	Important constituents	Sedimentary structures	Body and trace fossils	Taphonomy	Interpretation
Oolitic grainstone–packstones	Ooids (types 5, 3), peloids and coated grains, intraclasts, oncoids	Medium bedded, planar parallel laminae, planar tabular cross-stratification	Bivalves, Echinoids, spines, gastropods, corals, oncoids	Disarticulation, micritization, convex-up, not in situ	Shallow subtidal. Inner ramp
Mound	Colonial sponges, peloids, echinoderms, bivalves, gastropods, serpulids, bryozoan	Massive	Sponges, serpulids, forams, microbialites	Fragmentation, articulation, micritization	Sponge mound. Inner ramp
Coral boundstone	Bioclasts, peloids, intraclasts	Massive	*Actinastrea* sp., *Australoseris* sp., *Cteneostreon* sp., echinoderms, gastropods, serpulids, sponges, dasycladacean, cyanophytes (*Cayeuxia* sp.), forams, ostracods, bryozoans	Bioerosion, micritization, dissolution, recrystallization	Reef core. Inner ramp margin
Coral floatstone–rudstone	Ooids, bioclasts, peloids, intraclasts	Massive	*Actinastrea* sp., *Australoseris* sp., *Cteneostreon* sp., echinoderms, gastropods, serpulids, sponges, dasycladacean, cyanophytes, (*Cayeuxia* sp.), forams, ostracods	Fragmentation, bioerosion, micritization, poor sorting, dissolution, recrystallization	Back reef. Inner ramp margin
Algal boundstones MF-1	Peloids	Fine-to medium bedded, micro-teppe, mudcracks	Stromatolites, bivalves, ostracods, forams	Micritization, disarticulation, fragmentation	Upper intertidal-lower supratidal. Inner ramp
Peloidal wackestone MF-2	Peloids, ooids with fine radial structure	Fine bedded, massive to laminated	Bivalves, ostracods, forams, dasycladacean	Fragmentation, disarticulation, dissolution, molds filled by rims and granular calcite	Shallow subtidal. Inner ramp
Bioclastic wackestones MF-3	Bioclasts, ooids with fine radial structure, intraclasts, peloids	Fine bedded, massive to laminated	Bivalves, gastropods, forams ostracods	Fragmentation, disarticulation, incrustation, dissolution, molds filled by micrite or granular calcite	Shallow subtidal. Inner ramp
Bioturbated wackestones MF-4	Peloids	Fine bedded, massive to planar lamination. Horizontal bioturbation, nodular stratification	Bivalves, oncoids, gastropods, calcispheres, forams, dasycladacean, cyanophytes	Bioerosion, micritization, disarticulation, low abrasion	Shallow subtidal. Inner ramp
Bioclastic packstones MF-5	Bioclasts, peloids, intraclasts	Fine bedded, massive to planar lamination	Bivalves, oncoids, gastropods, forams, dasycladacean, cyanophytes (*Cayeuxia* sp.)	Disarticulation, low abrasion, bioerosion, micritization	Shallow subtidal. Inner ramp
Oncoidal packstones MF-6	Oncoids, ooids, bioclasts peloids, intraclasts	Fine bedded, massive	Oncoids, bivalves, echinoid spines, gastropods, corals	Disarticulation, low abrasion, bioerosion, micritization	Shallow subtidal. Inner ramp
Matrix-to clast supported carbonate breccia	Bioclastic packstones, oolitic grainstone–packstones, coral boundstones, silicified laminated carbonate clasts	Massive	Absent	Absent	Paleokarst

features described indicates that these packestone lithofacies are event deposits (Kreisa, 1981). The diverse fauna suggests that deposition occurred in a marine environment of normal salinity. Storm deposits that occur made up of packstone beds rich in gryphaeid shells entirely of amalgamated event deposits, followed

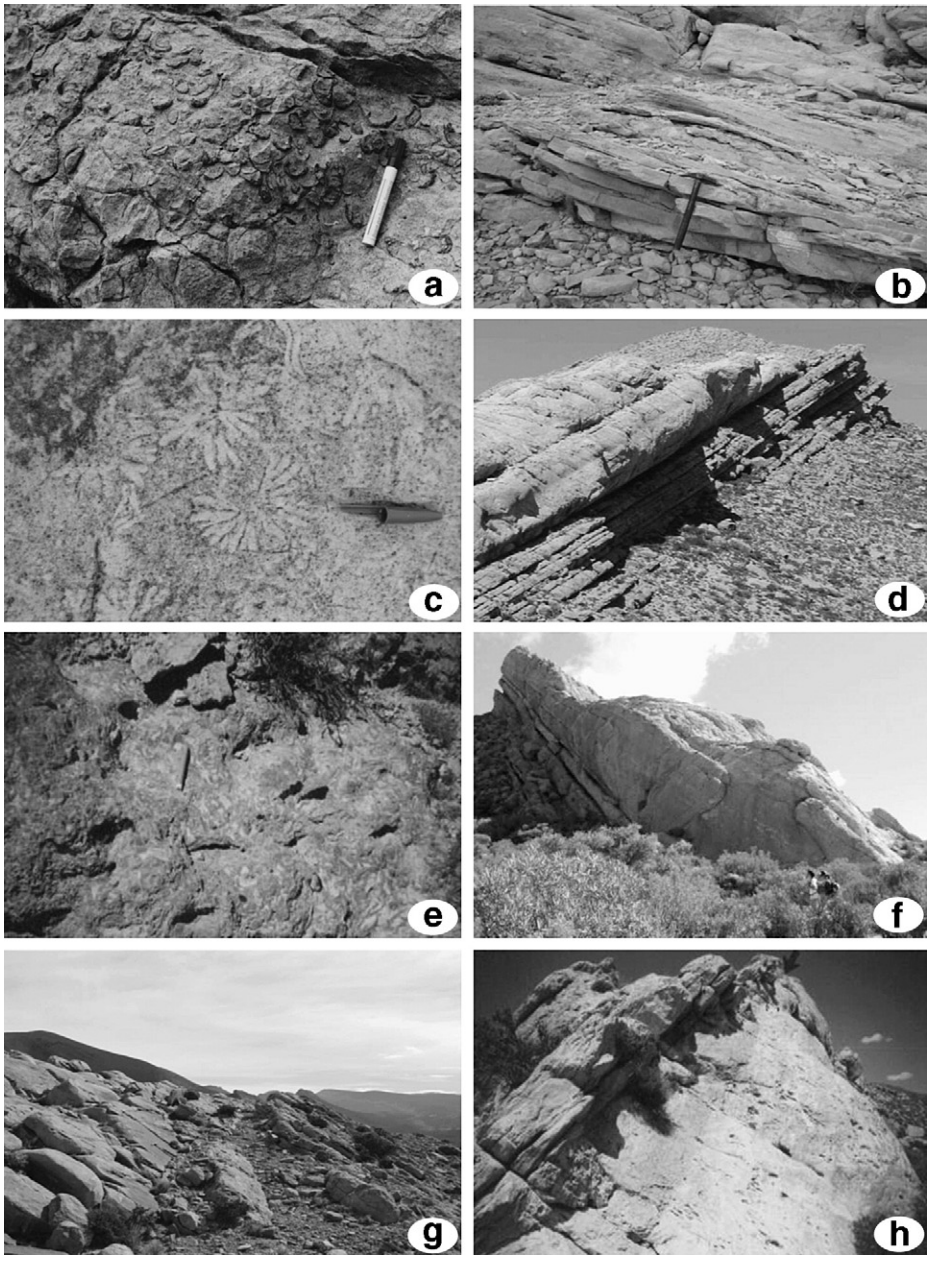

Fig. 5. (a) Outer ramp. Storm deposits at *Barda* 1 showing packstone with gryphaeids overlain by wackestone of fair-weather interval. Pen for scale: 15 cm. (b) Middle ramp: Hummocky cross-stratified grainstone–packstone. Hammer for scale: 33 cm. (c) Trace fossil *D. ottoi.* Scale: 4 cm. Inner ramp (oolitic shoal), (d) Outcrop photograph showing oolitic grainstone–packstone shoal underlying the inner ramp margin (patch reef); (e) Small sponge bioherm at the base of depositional facies. Pen for scale: 15 cm, (f). The upper most shallowing-upward succession of the depositional facies D. Notice the core reef facies represented by migrating buildups, (g). Outcrop of lagoonal deposits overlying the limestones shorefaces of middle ramp. Hammer for scale. 33 cm, (h) Blue horizontal level located in the karst facies. Notice the reef, karst and lagoon facies.

by wackestones with minor amounts of gryphaeid shells. They are characterised by sharp erosional bottom surfaces which are massive or with local grading.

These features record a decrease in physical reworking and suggest deposition in an environment below the fair-weather wave base. Often subject to the action of storm waves, or currents. Convex-up stacking of left valves is diagnostic of flows such as those generated by weak storm events (Kidwell and Holland, 1991) on the outer ramp (Kreisa, 1981; Aigner, 1982; Handford,

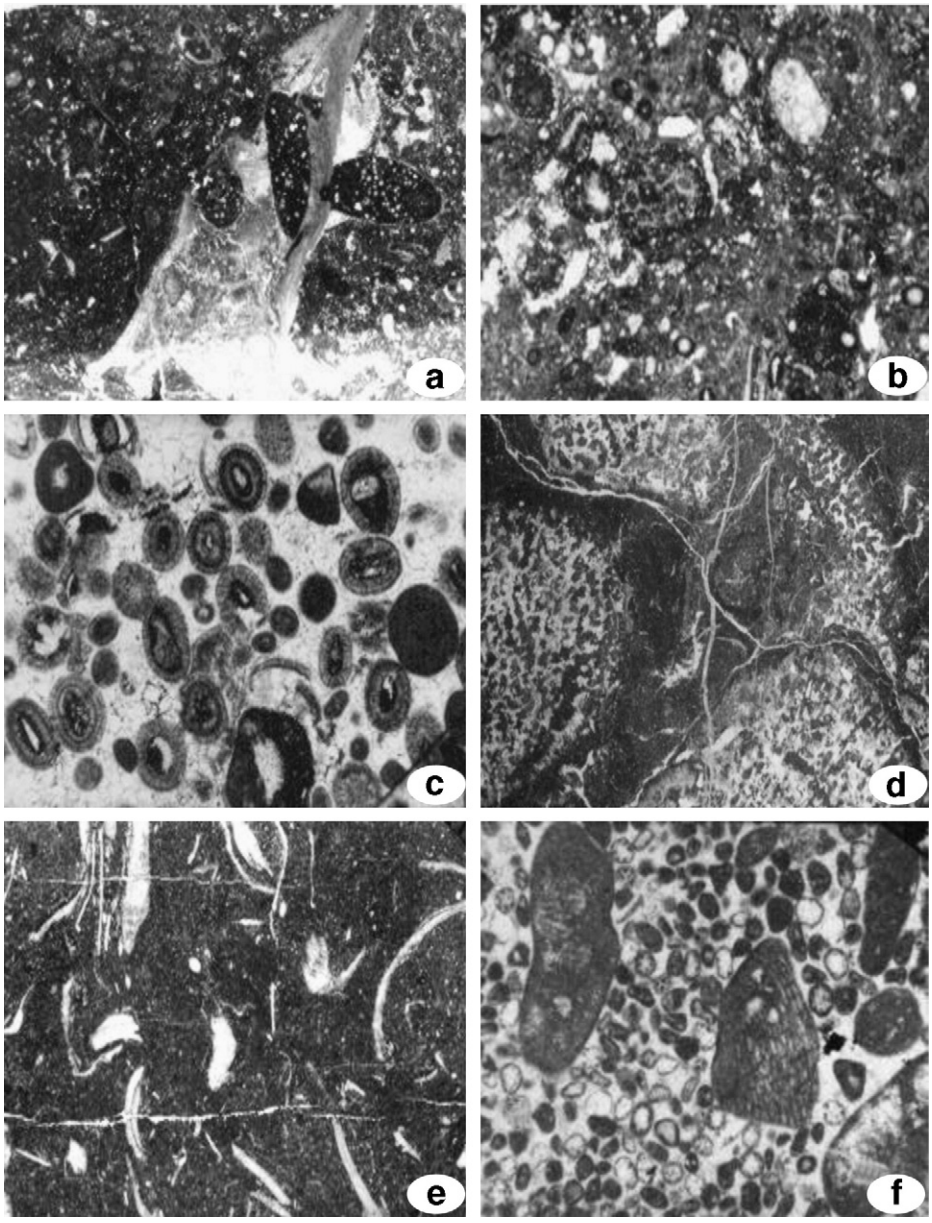

Fig. 6. (a) Bioclatic packstone (MF-1): fragment of gryphaeid shell with larger boring filled with micrite and small serpulids. ×10; (b) Intraclastic–bioclastic packstone (MF-2): subrounded intraclasts and scattered ooids and bryozoan fragments. ×25. (c). Different types of ooids. Notice the concentric and fibro-radial envelope. Intraclasts and micritized ooids also appear (×25); (d). Longitudinal section of sponge coated by microbialite crusts (×20); (e). Microphotograph from the peloidal wackestone microfacies. Notice peloids and bivalve shell fragments. ×20; (f). Microphotograph of bioclastic packstone showing fragments of *Cayeuxia* sp., oncoids and dasycladacean fragments. ×20.

1986). The biofabric becomes more dispersed upward and the shell beds become a loosely packed matrix supported wackestone.

The succeeding wackestone lithofacies displays fine parallel lamination and gradation indicating sedimentation from suspension in a low energy environment, as is likely on the outer ramp below the storm wave base. Sometimes the upper part is marked by cm-scale nodular wackestone facies (4–8 cm) composed of scattered molluscs shells. The nodular texture is possibly indicative of firmground development. No evidence of subaerial exposure is found.

Such event beds are represented by a parautochthonous skeletal concentrations of mixed biogenic–sedimentologic origin (Kidwell et al., 1986) produced by storm-currents flowing below fair-weather wave base

and giving rise to composite multiple-event shell concentrations (cf. Kidwell, 1991).

Widespread borings of the left valves indicate *post-mortem* bioerosion probably attributable to endolithic algae, bacteria or fungi, and the larger borings, to bivalve molluscs or sponges. High bioerosion indicates to long exposure on the sea floor during periods of low sedimentation rate after repeated processes of erosion, i.e., transportation during exhumation following each event.

These lithofacies were deposited on the outer ramp, below mean storm-weather wave base. Nevertheless the thin normally graded beds within this lithofacies may be attributed to storm processes. Storm waves and/or current action were likely responsible for the reworking and transport of shells and their mechanical breakdown, as is possible to observe in some level, where the fragmentation of shells is high. The upper limit of this carbonate unit is sharp and corresponds with the thickly-bedded packstone–grainstones which are assigned to the middle ramp.

3.2. Greyish grainstone/packstone—middle ramp (B)

These deposits consist of vertically stacked progradational packstone–grainstones and subordinate wackestones, siltstones and calcirudites. This lithofacies assemblage increases in thickness upwards and varies from 3.5 to 14 m. Previous studies of these section recognized some sandstone lithologies (Legarreta, 1991) but recent intensive study reveal that the detrital components only reached up to 35% (Palma et al., 2005).

The lithofacies is dominated by ooids, peloids, intraclasts, pelecypods, echinoderms, green algae, cyanophytes and gastropods. Accessory components include foraminifers, and isolate serpulids. Ooids in these lithofacies display five kinds of cortices. Some often with a darker nucleus consisting of peloids, small fragment of bioclasts or detrital particles. Many ooids have also been dissolved and their molds filled by single crystals of granular calcite. They include ooids type 1, 2, 3, 5 and superficial ones (cf. Strasser, 1986). Ooids type 1 are well rounded and intensively micritized. Ooids type 2 are elongated or irregular. Cortex layers show fine laminae mostly micritic. Ooids type 3 have a cortex composed of different thin laminae and fine radial structure, many of them are micritized in patch. Ooids type 5 exhibit a radial structure followed by an intensive micritization towards the surface of the particles. Superficial ooids are common and show only one or two thin micritic lamina. Eight lithofacies have been recognized based upon on their lithology, primary sedimentary structures, and especially the type of bioturbation. They include parallel-laminated packstones, wave ripples peloidal wackestones, planar cross-stratified packstone–grainstones, massive packstone–grainstones, swaley cross-stratified grainstone–packstones, hummocky cross-stratified grainstone–packstones, massive calcirudites, and siltstones lithofacies (Table 1).

3.2.1. Interpretation

These deposits are interpreted as a typical coarsening upward sequence which accumulated on a middle-ramp setting. The frequency of grainstone–packstones with HCS (Fig. 5b) and the spectrum of storm-bed thicknesses are thought to reflect depth, frequency of storm events and proximity to the source area (Aigner, 1985). In fact, oolitic–peloidal grainstone–packstone layers represent resedimentation of particles derived from nearby ooid producing shoal water environment (inner-ramp). Different cortical fabric of the ooids reflect changes of environmental conditions. In fact, ooids type 1 suggest a rapid deposition of the cortical layer and/or high energy (Strasser, 1986). In contrast, ooids type 2 suggest a lagoonal setting with growth of cyanobacteria, and as in case of ooids type 3 suggest intermittent growth with abrasion of the ooid surface as consequence periods of agitation (cf. Strasser, 1986). On the other hand, ooids type 5, with radial structure, indicates periods of normal turbulence. Meanwhile superficial ooids are indicative of a low water energy or probably the decreasing intensity of oolitization processes in more protected conditions. Peloids are subrounded by micrite, whereas some showing grain-supported texture (packstone) are the result of increased winnowing.

The presence of disarticulated and broken bioclasts as well as intraclasts are indicators of intense reworking and deposition from storm-induced currents transporting coated grains, and algae from the inner ramp shoal and lagoon, respectively. Further evidence for current induced deposition is provided by the erosive bases of these beds where scattered gryphaeid shell fragments and intraclasts are present.

The HCS units interbedded with siltstones suggest that higher energy conditions prevailed during the deposition of the HCS grainstone–packstones. Occasionally, fair-weather waves reworked the tops of the storm deposits and formed wave ripples (wackestone lithofacies), which are indicative of a gradual decrease of energy conditions, whilst the bioturbated siltstones represent quiet periods of slow deposition during fair-weather. The upward decrease in grain-size and the common upward increase in bioturbation suggest a reduction of the depositional rate such as provided by a waning of current energy in the

upper sediment surface. Bioturbation was extensively developed during the deposition of the siltstones.

HCS units formed as a result of the waning oscillatory flows, and waning of the combined oscillatory flow and unidirectional geostrophic currents created by periodic storm events (Dott and Bourgeois, 1982). Therefore the HCS grainstone–packstones are interpreted to represent deposition above storm wave-base in the lower shoreface, within a storm-dominated inner shelf setting (Hambling and Walker, 1979; Leckie and Walker, 1982; Cheel and Leckie, 1993). The amalgamated hummocky cross-stratified grainstone–packstones are interpreted as having been deposited in a middle shoreface environment, formed by repeated storm events. The amalgamated HCS beds and their lateral discontinuity are also features commonly reported in shallow water storm deposits (Kreisa, 1981).

The massive and bioturbated packstone–grainstones were probably deposited under alternatively high energy currents as suggested by fragmented shell accumulation at the base of the beds and periods of quiet conditions of slow deposition, which allowed the infaunal organisms to homogenize the substrate in the lower shoreface transition zone. Oxygenated bottom conditions are in general indicated by the presence of intense bioturbation. The thin calcirudite beds were produced by the erosion of the earlier shoreface deposits by current associated with storm conditions. Lenses of fragmented gryphaeid shells reflect storm reworking of bioclastic material locally derived. The poor sorting indicates that the deposition was rapid.

As indicated by their relationship with the above depositional facies and the underlying (HCS) lithofacies, the calcirudite beds suggest the superposition of storm beds, without the preservation of fair-weather deposits on the lower shoreface. The trace fossil association is characterized by the abundance of *Dactyloidites ottoi* (Fig. 5c) and *Gyrochorte* isp., which can be interpreted as a typical burrow of deposit feeders structures of the lower-middle shoreface zones (Howard and Frey, 1984). The observed trace fossils belong to the *Cruziana* ichnofacies. This ichnofacies is typical of subtidal zones below fair-weather wave base but above storm wave base (Frey and Seilacher, 1980).

According to different authors, various criteria have been used to identified the base of the shoreface zone. The base of the lower shoreface (*sensu* Reineck and Singh, 1980) is defined at the lowest fully amalgamated hummocky cross-stratified (HCS) grainstone–packstone lithofacies.

According to Kamola and Van Wagoner (1995) the base of the shoreface zone is the amalgamated beds with HCS. Others such as Walker and Plint (1992) consider the base of amalgamated beds with swaley cross-stratification (SCS), or the base of beds with tabular or trough cross-stratification as the base of the shoreface (Hampson and Storms, 2003). However, the predominance of HCS and sedimentologic characteristics allow us to interpret these sediments as having been deposited in the lower-middle shoreface setting.

The grainstone–packstones with swaley cross-stratification are indicative of storm-dominated deposition above fair-weather wave base in the upper shoreface setting (Plint and Norris, 1991). Occasional horizontal bioturbation on the top of SCS reflects minor reworking during periods of quiescence.

The packstone–grainstones with planar cross-stratification represent energetic shallow water depositional conditions and product of migrating megaripples. These lithofacies reflect alternating episodes of siliciclastic and carbonate deposition. The differences in hydraulic equivalence led to the segregation of the two sediment types during deposition. The repetitive alternation of both siliciclastic and carbonate dominated laminae can be interpreted as a product of both particles and erosion of nearshore siliciclastic deposits and subtidal carbonates.

The increase in grain size and abundance of detrital particle indicates an increase in both energy and supply of siliciclastic material southward. The paucity of bioclasts in this lithofacies suggests that unfavorable conditions existed for the fauna because of increased reworking of the substrate and the influx of siliciclastic material.

The abundance of vertical-burrow-dominated trace fossil characteristic of the *Skolithos* ichnofacies in these deposits is indicative of deposition in a moderate to high-energy setting. The *Skolithos* ichnofacies reflect the activities of organisms under intense water circulation, and an unconsolidated grained substrate (MacEachern and Pemberton, 1992). *Skolithos* support a nearshore, upper shoreface to possible lower shoreface setting (Curran, 1985).

From the above observations and interpretations of the succession of sedimentary facies, these sediments are characteristic of middle-ramp storm-dominated shoreface deposits, similar to the examples described by Aigner (1985). The predominance of HCS and SCS and local tabular cross-stratification suggests that most of the shoreface were susceptible to combined flow directions with dominant storms processes.

3.3. Oolitic grainstone—inner ramp (C)

These deposits consist of light grey, generally well-sorted grainstones with locally subordinate packestones (Fig. 5d). Ooids, peloids, and coated grains are dominant

as well as skeletal fragments (Table 2). Different types of ooids occur (Fig. 6c): those affected by a strong micritization, and those with two or three nuclei, which are represented by ooids with a fine radial structure, and locally display micritization. Some superficial ooids are also present. Oncoids range in shape and consist of relatively smooth concentric laminae to highly irregular growth structures.

Small sponges bioherms (Fig. 5e), 10 to 30 cm in height, appear on the base of this shallowing-upward succession (Fig. 5d) (Palma et al., 2003, 2004). They are composed exclusively of Hexactinellida sponges and laminated peloidal carbonate crusts. Microbialites with dome shape or branch upwards bind the sponges (Fig. 6d), which are encrusted by organisms such as serpulids, bryozoans and foraminifers. The presence of borings of lithophagus suggests that the microbial crusts were lithified early.

3.3.1. Interpretation

The presence of a grain-supported fabric as well as ooids, peloids, coated grains and fossils content suggest a high energy and shallow-water depositional setting in the inner ramp for these lithofacies. The complex oolites and oncoids with concentric laminae, and an irregular or asymmetric growth structure suggest that deposition occurred mainly under a relatively high-energy environment (Peryt, 1983). Oncoids commonly occur in a wide range of platform facies but are most common in grainstones and packstones when the platform was prone to wave- and current action. Oncoids in platform facies are commonly restricted to the upper portions of shoaling-upward cycles (Eberli and Ginsburg, 1987).

The presence of oolites envelopes such as oolites with fibro-radial and concentric structures (types 5 and 3, respectively from Strasser, 1986) and those with complex and superficial ones indicate different environmental conditions. As reported by Strasser (1986), fibro-radial and concentric structures of some ooids indicate a restricted lagoon affected by a low to intermittently agitated energy marine environment, but the presence of intraclasts of the same microfacies indicates early cementation and reworking with an intraformational source, suggesting that the calm water conditions were not continuous. The presence of borings of lithophagus in the microbialites suggests that the microbial crusts were lithified early.

3.4. Grey and white coralline limestones—inner ramp margin D

This facies consists of *in situ* reef framework coral boundstones and back reef facies that occur along the inner ramp margin (Table 2). The build-up was formed on the top of a shallowing-upward succession and reaches a thickness of 20 m (Fig. 5f).

This core-reef facies is composed of a white unstratified coral limestone dominated by branching and domal coral in growth position. Some small coral-sponge bioherms with notable microbial fabrics variable in sizes and forms were recognized by Palma et al. (2004). The grades of smoothening on individual coralla surfaces vary among grade 2 and grade 4 in Ketcher and Allmon's (1993) classification; meanwhile, variation of bioerosion on coralla surfaces is between grade 1 to grade 2 (Ketcher and Allmon, 1993). The matrix between colonies is composed mainly of bioclastic wackestones and packstones with some ooids and coated grains. The bioclastic material consists of abundant fragments of the reef-frame builders (Table 2).

The back-reef facies consists of coral floatstone–rudstone containing abundant fragments of branching corals with fragments varying in size from 2 to 50 cm, with poor bedding and sorting. They appear interbedded with fossiliferous wackestone–packstone–grainstones with similar microfauna.

The reefs are underlain by the paleokarst facies or subtidal wacke/packstones from the lagoonal deposits.

3.4.1. Interpretation

The reef-core exhibit very low diversity of scleractinian corals (cf. Morsch, 1990). The coral fauna, in particular the dominance of branching forms, is indicative of shallow well illuminated waters (Morsch, 1990; Insalaco, 1996). The abundant associated fauna represents a benthic community that included suspension feeders, grazing herbivores and scavenger organisms and is suggestive of poor oxygenated conditions. Bioclasts are highly micritized, due to their exposure on sediment surface for a considerable amount of time.

The different species of gastropods and bivalves indicate clear and turbulent waters (Dodd and Stanton, 1981), and the coral morphology suggests a moderate to high-energy environment and a variable sedimentation rate (James, 1983; Tucker and Wright, 1990). Moreover, grazing gastropods suggest the presence of algal mats, which are a common micrite producer (Bathurst, 1976). Such microbialites associated with coral-sponges and other microencrusters such as bryozoans, serpulids and foraminifers are related to conditions of high nutrient available (Leinfelder, 1992). There is no evidence of a persistent barrier and they probably formed small patches on the contemporary sea floor (cf. James, 1983). From a taphonomic point of view, the smoothened coral could be related to biotic or abiotic processes, but is

difficult to recognize such biotic ones. Meanwhile abiotic processes such as dissolution and probably abrasion seem more likely.

The faunal assemblage of the back-reef facies and its type of preservation suggest limited transport from a shallow water moderate to high energy environment, which was intensive reworked by currents or storms. The presence of small coral colonies in the growth position suggests a close relationship between the reef and lagoon environments.

3.5. Carbonate wackestone–packstone—inner ramp (E)

The lithofacies (Fig. 5g) includes bioturbated wackestones, peloidal wackestones, bioclastic wackestone–packstones, oncoidal packstones and floatstone/rudstones rich in bioclastic debris (Table 2). Beds are usually sheet-like and laterally discontinuous. It overlies the packstone–grainstone of the middle ramp or the paleokarst level. In both cases these deposits have bioclastic floatstones or rudstones at their base. It is usually 30 to 60 cm thick and is often laterally discontinuous.

On the basis of particles, textures and biota, six microfacies types have been identified in these deposits: algal boundstone (MF-1), peloidal wackestone (MF-2), bioclastic wackestone (MF-3), bioturbated wackestone (MF-4), bioclastic packstone (MF-5), and oncoidal packstone (MF-6), (Fig. 6e, f).

3.5.1. Interpretation

Based on the presence of very thin and irregular laminae, that are locally domed, and the similarity of peloidal or clotted microtextures with those observed in stromatolites by Riding (2000), the laminated rocks are interpreted as cyanobacterial laminites or stromatolites (MF-1). The character of this facies suggests an upper intertidal to lower supratidal depositional environment, as indicated by the presence of tepee structures, isolated mud cracks and the highly continuous laminae with alternating colours (Shinn, 1983a,b; Scoffin, 1987). Micro-tepee structures and isolated mud cracks interrupt the deposition and suggest repeated periods of emergence and subaerial exposure. Such stromatolites are restricted to the lagoonal facies and are commonly found at the top of shoaling-upward cycles indicating progradation of peritidal environments into the platform lagoon (Emery, 1996).

The composition of the peloidal wackestone (MF-2) suggests deposition in a lagoon characterized by calm water with the presence of small ooids, indicating episodic influence of waves.

Because of the increase in fossil content, the bioclastic wackestone microfacies (MF-3) is thought to have formed in a shallow marine setting located not far from the site of peloidal wackestone microfacies deposition. Small intraclasts consist of bioclastic wackestone and peloidal wackestone. The presence of ooids suggests that they have been transported from their normal high-energy environment and deposited in the relatively low energy environment of a lagoon.

The characteristics of the bioturbated wackestone (MF-4) indicate deposition under quiet water oxygenated conditions as suggested by the abundant traces of bottom dweller in a protected shallow water marine environment.

As implied by the abundant fossil content, the bioclastic packstone (MF-5) was deposited under moderate-energy lagoon setting. Dasycladacean algae and *Cayeuxia* sp., are generally regarded as indicator of a lagoonal environment.

The presence of grain-supported textures as well as oncoids, ooids, fossil content and intraclasts in the oncoidal packstones microfacies (MF-6) suggest a high-energy and shallow-water depositional setting. The structure of the oncoids and their frequent association with a high degree of fragmentation and rounding of bioclasts also suggest a high-energy environment with frequent reworking.

3.6. Carbonate breccia—paleokarst (F)

This consists of stratified breccia (Fig. 5h) and shows an irregular relationship with the underlying facies, represented by bioclastic packstones, oolitic grainstones and coral reefs, which themselves are organized in a shallowing-upward sequence.

The thickness of the breccia is variable ranging from a few centimeters up to 1.3 m. The fabric is disorganized without any clast orientation, and does not show any internal stratification. Both matrix and clast supported fabrics are present. There is no relationship between fabrics and clasts size. Clasts are polymictic, reflecting derivation from bioclastic packstones, oolitic grainstones and coral limestone facies. Clast size range from 1.5 to 30 cm but locally large clasts were observed. They are highly angular and the sorting is poor. Clast shape is variable, but blades to rods are very common forms.

Vertical fissures extend up to 50 cm downward from the breccia surface. They have planar or slightly curved boundaries, and are filled up with carbonate clasts of similar composition to those found in the breccia.

Small dissolution pockets of breccia occur such as silicified laminated carbonate clasts derived from the local carbonate bedrock. The silicification was intense and consists of chalcedony and euhedral quartz.

3.6.1. Interpretation

The paleokarst is represented by a stratified breccia (Table 2) and shows an irregular relationship with the underlying facies, represented by bioclastic packstones, oolitic grainstones and coral reefs, which themselves are organized in a shallowing-upward sequence.

The thickness of the polymictic breccia is variable ranging from a few centimetres up to 1.3 m. The fabric is disorganized without any clast orientation, and does not show any internal stratification. Both matrix and clast supported fabrics are present. Clast size range from 1.5 to 30 cm but locally large clasts were observed.

Vertical fissures extend up to 50 cm downward from the breccia surface, and small dissolution pockets of breccia occur such as silicified laminated carbonate clasts derived from the local carbonate bedrock.

This lithofacies is interpreted as the results of an episode of emergence and karstification due to a sea-level fall and a stratigraphic break (148 Ma; Legarreta, 1991) which is well developed throughout the area, from the Bardas Blancas section, 60 km southward to the Sierra Azul outcrops. Similar paleokarst features affecting identical facies can be recognized in other part of the basin (Lo Forte and Palma, 2002) but lack of biostratigraphical control does not allow us to correlate over the area of this major break.

A pale blue horizontal horizon cut the upper rocks of the last facies affected by the paleokarst. A detailed petrographic analysis (Palma et al., 2002) of this level showed the passage from marine–phreatic diagenesis to meteoric–phreatic conditions related to the position of the water table, and is similar to the examples described by James and Choquette (1984).

Small scale dissolution features are related to evidence of pre-compaction leaching of allochemical particles such as molluscs, corals and some ooids, which are now filled with druse calcite and granular calcite cement. Isotopic data from granular calcite crystals show variations in $\delta^{18}O$ from − 6.3 to − 9.3, which suggest origin from meteoric waters (Palma et al., 2002). Fissures of the rock probably are the product of solution associated with water circulation on the paleokarst surface (Sweeting, 1973).

4. Depositional sequences

The Upper Callovian–Oxfordian sedimentary succession in the Bardas Blancas area shows, at least, four important discontinuities which can be followed laterally tens of kilometres. These discontinuities clearly separate depositional units that in Bardas Blancas area constitute four third-order depositional sequences comparable to those described by Van Wagoner et al. (1988) and Legarreta (1991).

A general attempt have been mainly made by Legarreta (1991) and Legarreta and Uliana (1996) in the west-central Argentina area to define depositional sequences for the whole Jurassic. The sediments of the six depositional facies described in the previous chapter of this work broadly correspond to 2nd, 3rd and 4th sequences of La Manga Formation described by Legarreta (1991). In the present paper, the six depositional facies units are combined into three depositional sequences (DS-1, DS-2 and DS-3) (Figs. 4 and 7) according to the depositional sequence concept of Vail (1987) and following the depositional systems tracts philosophy of Haq et al. (1987), Vail (1987), and Bally (1987).

4.1. Depositional sequence 1 (DS-1)

The DS-1 shows an important erosive surface at both its base and top and crops out only partially in the study area. It reaches its maximum thickness in *Barda* 1 and thins progressively northward to *Barda* 4, where it is difficult to recognize. The base corresponds to a sequence boundary (SB-1) (Fig. 4), probably related to the intra-Callovian discontinuity. Below this surface is a stack of 17.8 m thick of conglomerates consisting of by 1 m thick fining-upwards sequences of subrounded volcanic clasts (Fig. 4). This conglomerate level appears at *Barda* 1 and locally at *Barda* 4. At *Barda* 1 where also pinch out laterally, reaching up 305 m wide and has a general concave morphology.

DS-1 consists of only depositional facies A (greyish wackestone/packstone) that only represents part of the highstand systems track (HST-1) of the whole sequence, while the remainder was either not deposited or has been eroded.

4.2. Depositional sequence 2 (DS-2)

The DS-2 develops on SB-2. The process or processes that created the SB-2 erosive surface still remain unclear. Although a fall of sea-level is the most likely cause, field evidence is inconclusive as to whether or not either the shelf or the shelf margin was exposed. The lower part has an abrupt contact with underlying deposits (SB-2), characteristic of a rapid sea-level rise, and represented by depositional facies B (greyish grainstone–packstone). It consists of a transgressive systems tract (TST-2) (Fig. 4) that is thinnest towards the inner platform margin while it thickens basinward. This sequence develops on a transgressive surface 2 (Ts-2) with packstone–grainstone. These sediments are also

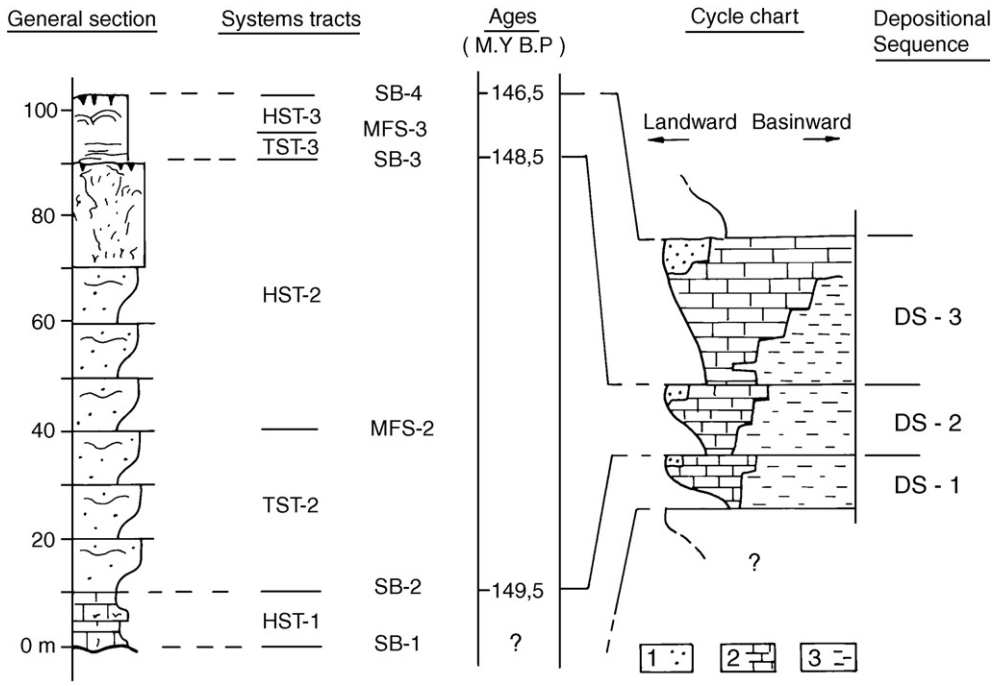

Fig. 7. Sketch of the three studied depositional sequences and their differentiated systems tracts for a general section of the studied La Manga Formation. 1—shallow marine, 2—marine carbonates, 3—basinal.

evidence of clear retrogradation with the presence of small sponges and corals fragments as well as transgressive facies in the basinward area directly deposited on the Ts-2. Oolitic grainstones, floatstones and rudstones rich in coral fragments represented by depositional facies (oolite grainstone) constitute the upper part of the TST-2 in *Barda*-3 and *Barda*-4. This oolite grainstone facies did not reach the margin (*Barda*-1 and *Barda*-2) during the transgressive event (Fig. 4) which developed a surface of transgressive erosion or a ravinement surface (Swift, 1968) which is more incised landward (Fig. 7).

The ultimate deepening stage of DS-2 is represented by the maximum flooding surface 2 (MFS-2). This surface, probably very extensive (>100 km) in a N–S direction, represents a regional paraconformity that was buried by downlap deposition of the highstand system tract 2 (HST-2). This surface separates in the study area depositional facies C (oolite grainstone) facies below from depositional facies D (grey and white coralline limestone—inner ramp margin) facies above, except for the landward area (*Barda*-1), where a high sea-level period still preserved packstone–grainstone of depositional facies B deposited both below and above the MFS-2, becomes exclusively carbonate sedimentation basinward. MFS-2 is the boundary between a transgressive unit or retrogradational body of depositional facies C (oolite grainstone) and the lower part of depositional facies B (greyish grainstone–packstone) and an overlying regressive unit or progradational body represented by depositional facies D (grey and white coralline limestone—inner ramp margin) and the upper part of depositional facies B.

Highstand progradation (highstand systems tract 2, HST-2) in the study area brought middle-ramp storm-dominated shorefore deposits represented by depositional facies B (greyish grainstone–packstone) to a position approximately 2 km shelfward of the landward limit of underlying TST-2. The new shelf scenario was dominated by a carbonate bank showing aggradational characteristics during the first stages of the deposition of depositional facies D (grey and white coralline limestone—inner ramp margin), while in a second stage of the HST-2 the shelf changed in character towards the margin to an aggradational–progradational situation.

Basinwards, the reef margin does not appear to have been steep according to field observations in *Barda*-4 area. This could be due to the absence of a real reef barrier. However, the platform probably developed a very flat top at or around sea-level, as indicated by the effects of karstification at the top of depositional facies D (grey and white coralline limestone—inner ramp margin) over large part of the study area. Karstification development (depositional facies F, carbonate breccia) could be related to rapid sea-level drop preventing

deposition. This processes mark the upper part of DS-2 and the beginning of the DS-3.

4.3. Depositional sequence 3 (DS-3)

The DS-3 is less developed than DS-2 and never reaches more than 22 m thickness in the outcrops. This sequence starts on SB-3, a boundary representing the flooding surface between the HST-2 and the overlying TST-3 of the new DS-3. This surface is a type 3 sequence boundary (of Schlager, 1999) and is well-developed on the drowned reef of *Barda*-3 and *Barda*-4. This new highstand–transgressive systems tract (HST-3–TST-3) boundary indicates again a major stratigraphic turning point and a new level of reorganization of the sedimentation pattern related to the drowning of the carbonate platform and the subsequent continental influence (Figs. 4 and 7).

The lower part of DS-3 is here represented by TST-3. As in the case of the previous DS-2, basinward lowstand-deposits DS-3 are not recognized in the study area probably due to the platform morphology (cf. Schlager, 1989). TS-3 is characterized by a clear retrogradation of rounded bioclastics facies and the presence of a transgressive facies including sponge mounds located basinward, in the area of *Barda*-4. The presence of the sponge bioherms with microbialites suggests a low sedimentation rate.

The transgressive tract seems not to have developed uniformly as it is interrupted by two small paleokarst levels that can be followed discontinuously throughout the study area (Fig. 7), similar way to the ones described during the lower transgressive stage of the Middle Triassic carbonate ramp systems of the Catalan Basin by Calvet et al. (1990). In both cases, sporadic phreatic incursions interrupted the development of the lagoon facies.

The maximum deepening corresponds to the discontinuity surface, here represented by MFS-3, which separates TST-3 from HST-3. Lagoon facies of depositional facies E (carbonate wackestone/packstone) which were deposited during the highstand stage were probably isolated from the adjacent basin areas by belts of oolitic shoals which allowed the development of shallow water stromatolites. Small reefs from this unit were probably also located basinward of the oolite shoals but near to these latter ones. Relative fall in sea-level at the top of DS-3 could have caused the abandonment of surface shoals as described for the late Dinantian bioclastic shoals by Gawthorpe and Gutteridge (1990). Erosion was not the only process affecting the upper DS-3 as karstification developed again at the top of *Barda*-3(S) and *Barda*-3(N) and the top of this depositional sequence that corresponds to SB-4 (Fig. 4).

5. Depositional system evolution

The Oxfordian–earliest Kimmeridgian interval was a period of an important tectonic inversion in the Neuquén Basin. This was related to the fragmentation of the southwestern Gondwana and the opening of the Atlantic (Vergani et al., 1995). As subsidence was very slow during that time, eustatism resulted in important changes in the average position of the shoreline and was the most important control on sedimentary accumulation. In the general depositional trend, La Manga Fm. is included in a flooding stage after an Early-Middle Callovian emergence and before shallowing and desiccation during the Early Kimmeridgian (Legarreta, 1991; Legarreta and Uliana, 1996). The three described depositional sequences would correspond to 3rd order depositional sequences constituted by different parasequences, probably indicating smooth short term sea-level changes with change in shelfal accommodation (Duval et al., 1992).

Vertical and lateral lithofacies stacking patterns are here interpreted as recording gradual inundation and flooding of this northern area of the Neuquén Basin during the Oxfordian. This resulted in very much smaller platform and the margin steepening with rapid deposition. The lithology-specific effects on relief are small in this setting, and changes in input pattern or sea-level signals dominate the record (Schlager, 1989; Emery, 1996).

Fig. 8 shows a tentative schematic model of what could have been the response of the studied ramp and the types of sedimentary architecture produced by sea-level changes. Due to reduced oversteepened relief preserved in this basin (Mitchum and Uliana, 1985), the relative fall of sea-level, represented by the conglomeradic sediments in a stage previous to depositional facies A (greyish wackestone/packstones) sedimentation represents an event much like others in the general succession with an exposed portion of the ramp and basinward siliciclastic sediment supply (Fig. 8a). An erosive surface was probably related to sea-level fall which interrupted the development of depositional facies A. This stage was followed by a first stage of rapid sea-level rise with landward migration of a platform facies represented by depositional facies B and C (Fig. 8b). A retrogradational system developed with packstone–grainstone middle-ramp storm dominated shoreface deposits belts migrating landward and reducing protected areas to small isolated lagoons.

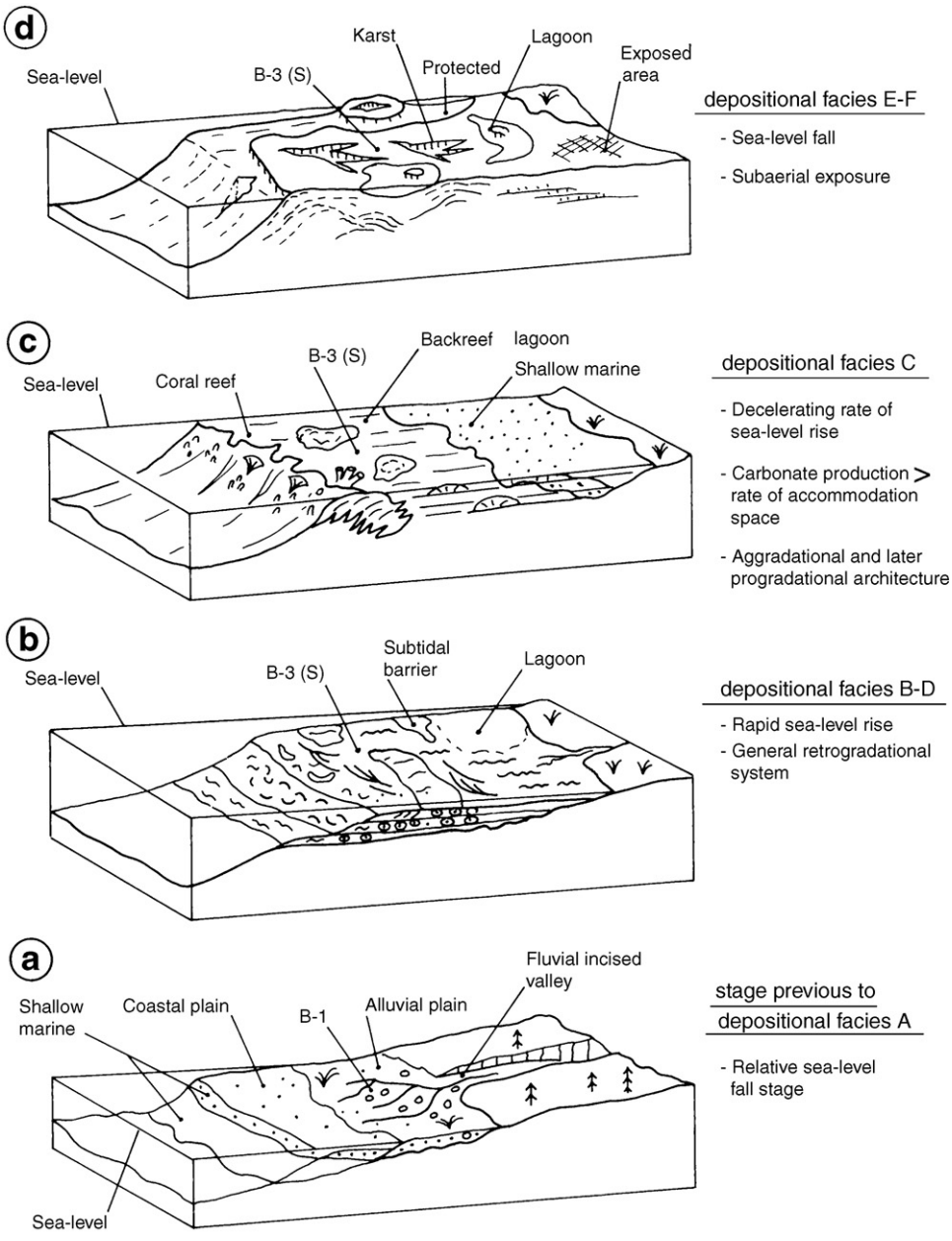

Fig. 8. Fourfold tentative paleoenvironmental reconstructions of the six depositional facies differentiated for the studied area. B-1 to B-3(S) represent *Barda*-1 and *Barda*-3 (south) respectively (see Figs. 1 and 4 for their location).

Different sets of the retrogradational system thicken shelfward and they thin by onlap at the base. It is very well seen in *Barda*-1 area where shoreface deposits cover the well-marked erosive surface that represents SB-2 and thin upwards. As sea-level continued to rise the former coastal plain or eroding shelf experienced a marine transgression and progressive water deepening until a highstand was reached, represented by depositional facies D (Fig. 8c).

This new stage introduced modifications in the geometry of the platform as reef belts developed and carbonate production was higher than rate of accommodation space. Rate of sea-level rise experienced a deceleration resulting in a thick aggradational and later progradational architecture of the morphology of the ramp (cf. Eberli and Ginsburg, 1987), as shown by the growing of the reefs in *Barda* 4 (Fig. 5f). Under these circumstances, carbonates were deposited in

neighbouring areas, including deeper waters to landward. The result of this stage was a widespread ramp that probably developed during the late part of the eustatic rise, the eustatic stillstand and during the early part of the eustatic fall. The ramp was under stress during this period as reefs started to develop in a wider area that finally reached *Barda*-3 (S), *Barda*-3 (N) and *Barda*-4 resulting in a backstepping favoring ramp development.

There was a sudden downlapping with landward erosion during the forced regression of a falling stage that represented the end of DS-2. This new sea-level fall resulted in widely exposed areas that suffered karstification represented by depositional facies F (carbonate breccia) (Fig. 8d). Karstification was well developed on the top of some reefs of the previous sequence, especially in those of *Barda*-3 (S) and *Barda*-3 (N). It indicates that there was selective action under a humid climate by acidified meteoric waters which probably affecting the topographically highest areas that could have laterally coexisted with simply exposed and reduced lagoon areas. Successive levels of solution notches were probably produced at ramp margins at the marine phreatic–meteoric interface (cf. Grammer et al., 1993).

A new landward extension of the platform environment flooded the exposed area. This retrogradational system of limestone shoreface facies was very short and rapidly changed to the development of lagoonal shallow subtidal and intertidal environment (depositional facies E, carbonate wackestone/packstone) related to decelerating rate of sea-level rise. The whole succession represents DS-3 and that which concluded with subaerial exposure and karstification. In the study area (*Barda*-1) at the top of La Manga Formation are veins and brecciated layers occur composed of barite and limestones fragments. Several stratabound barite and celestite deposits occur in the Neuquén Basin at different stratigraphic levels, where Brodtkorb and Barbieri (1993) recognized evidence of karstification and dissolution in level associated with evaporites.

After deposition of SD-3, the Neuquén Basin experienced a drastic change in pattern of deposition. A thick pile of evaporites (Auquilco Fm.) covered the basin. This new basin configuration could have resulted from extensional stress fields related to fragmentation of southwestern Gondwana and the Atlantic opening (Vergani et al., 1995).

6. Conclusions

Six depositional facies have been recognized in five complete sections in the upper part of the Oxfordian La Manga Formation in Bardas Blancas area, north of Neuquén Basin, west-central Argentina. The six defined depositional facies have been included into three third-order depositional sequences (SD-1 to SD-3), broadly equivalent to those of Legarreta's (1991) 2nd to 4th sequences. Recognized facies and microfacies allowed the differentiation of several carbonate marine ramp systems environments, including external-middle carbonate ramp with storm-dominated lower-middle shoreface deposits, patch reef, karst and lagoon.

Depositional sequences divided by systems tracts mainly represented by transgressive and highstand systems tracts stages are well developed throughout the studied area. Sequence boundaries are clearly of regional importance, as shows SB-1, probably related to the Intra-Callovian discontinuity and SB-2, SB-3 and SB-4 strongly marked by erosion and karstification.

The general depositional evolution during the slow subsidence experienced during the Oxfordian–earliest Kimmeridgian, is related to important tectonic inversion in the Neuquén Basin and the fragmentation of the southwestern Gondwana and the Atlantic opening.

A fourfold tentative architectural and sedimentary schematic model of the response of the ramp to sea-level changes is proposed. This model shows vertical and lateral lithofacies stacking patterns indicating reduced platform oversteepening shown by the small lithological effects on relief, where changes in input pattern or sea-level signals dominated the record.

Acknowledgements

This research was founded by the Universidad de Buenos Aires (grant n° x-133), the Consejo Nacional de Investigaciones Científicas y Técnicas (CONICET) (grant-PIP 02139) and Project CGL2005-01520/BTE of the Spanish Ministry of Research. We appreciated detailed suggestions made up by Graham Evans (Southampton University) and Leonardo Legarreta (Patagonia Exploración–Argentina). Javier Martín-Chivelet (UCM), G. Lo Forte, S. Lanés, L. Crousse, E. González and D. Kietzmann (UBA) were valuable field assistants. We wish specially to thank L. Buatois, G. Mángano for identifying the ichnofossils. The authors are also grateful to the authority of the Recursos Naturales de la Provincia de Mendoza-Delegación Malargüe for the assistance during the field work. Finally we want to thank M. Escudero (UCM) for the printing of the figures, Mr. Sepúlveda for his hospitality at Potimalal and Mr. J.C Poblete for driving the car and share his time with us in some remote roads of north Neuquén Basin.

References

Aigner, T., 1982. Calcareous tempestites: storm-dominated stratification in Upper Muschelkalk limestones (Middle Trias, SW Germany). In: Einsele, G., Seilacher (Eds.), Cyclic and Event Stratification. Springer, Verlag, Berlin, pp. 180–198.

Aigner, T., 1985. Storm depositional systems: Dynamic stratigraphy in modern and ancient shallow marine sequences, Lecture Notes in Earth Sciences, n°. 3. Springer–Verlag, Berlin. 174 pp.

Bally, A.W., 1987. Atlas of seismic stratigraphy vol. 1. Am. Assoc. Pet. Geol. Stud. Geol. 27.

Bathurst, R.G.C., 1976. Carbonate sediments and their diagenesis—developments in sedimentology 12. Elsevier, New York. 658 p.

Brodtkorb, M.K., Barbieri, M., 1993. Jurassic barite and celestine deposits of Neuquén Province, Argentina. Procc. of the 8th IAGOD Symposium, Stuttgart, pp. 243–254.

Calvet, F., Tucker, M., Henton, J.M., 1990. Middle Triassic carbonate ramp systems in the Catalan Basin, northeast Spain: facies, systems tracts, sequences and controls. In: Tucker, M., Wilson, J., Crevello, P., Sarg, J., Read, F. (Eds.), Carbonate Platforms, Facies, Sequences and Evolution. Int. Ass. Sedimentol., Spec. Publ., vol. 9, pp. 79–108.

Cheel, R.J., Leckie, D.A., 1993. Hummocky cross-stratification. In: Wright, V.P. (Ed.), Sedimentology Review, vol. 1. Blackwell Scientific Publications, Oxford, pp. 103–122.

Curran, H.A., 1985. The trace fossil assemblage of a Cretaceous nearshore environment: Englishtown Formation of Delaware, USA. In: Curran, H.A. (Ed.), Biogenic structures: Their Use in Interpreting Depositional Environments. SEPM Spec. Public., vol. 35, pp. 261–276.

Dellapé, D.A., Mombrú, C., Pando, G.A., Riccardi, A.C., Uliana, M.A., Westermann, C.E.G., 1979. Edad y correlación de la Formación Tábanos en Chacay Melehue y otras localidades de Neuquén y Mendoza. Con consideraciones sobre la distribución y significado de las sedimentitas Lotenianas. Obra Centenario Museo La Plata, vol. 5, pp. 81–105.

Digregorio, J.H., Uliana, M.A., 1980. Cuenca Neuquina. In: Turner, J.-C. (Ed.), II Simp. Geol. Regional, vol. 2. Acad. Nac. Cs. Córdoba, Argentina, pp. 985–1032.

Dodd, J.R., Stanton Jr., R.J., 1981. Paleoecology concepts and applications. John Wiley and Sons. Inc., New York. 559 p.

Dott Jr., R.H., Bourgeois, J., 1982. Hummocky cross-stratification: significance of its variable bedding sequence. Geol. Soc. Am. Bull. 93, 663–680.

Duval, B., Cramez, C., Vail, P.R., 1992. Types and hierarchy of stratigraphyc cycles. In: Centre Nat. Rech. Sci (Ed.), Mesozoic and Cenozoic Sequence Stratigraphy of European Basins International Symposium. Dijon, France, pp. 44–45. Abstracts.

Eberli, G.P., Ginsburg, R.N., 1987. Segmentation and coalescence of Cenozoic carbonate platforms, northwestern Great Bahama Bank. Geology 15, 75–79.

Emery, D., 1996. Carbonate systems. In: Emery, D., Myers, K.J. (Eds.), Sequence Sratigraphy. Blackwell Science, Oxford, pp. 211–237.

Frey, R.W., Seilacher, A., 1980. Uniformity in marine invertebrate ichnology. Lethaia 13, 183–207.

Gawthorpe, R.L., Gutteridge, P., 1990. Geometry and evolution of platform marine bioclastic shoals, Late Dinantian (Mississippian), Derbyshire, UK. In: Tucker, M., Wilson, J., Crevello, P., Sarg, J., Read, F. (Eds.), Carbonate Platforms, Facies Sequences and Evolution. Int. Ass. Sedimentol. Spec. Publ., vol. 9, pp. 39–54.

Grammer, G.M., Ginsburg, R.N., Harris, P.M., 1993. Timing of deposition, diagenesis, and failure of steep carbonate slopes in response to a high-amplitude/high-frequency fluctuations in sea-level, tongue of the Ocean, Bahamas. In: Loucks, R.G., Sarg, J.F. (Eds.), Carbonate Sequence Stratigraphy. Am. Assoc. Petrol. Geol. Mem., vol. 57, pp. 107–132.

Groeber, P., 1946. Observaciones geológicas a lo largo del meridiano 70. Hoja Chos Malal. Asoc. Geol. Arg. Rev., vol. 1, pp. 177–206.

Groeber, P., Stipanicic, P.N., Mingramm, R.G., 1953. Mesozoico. In: Soc. Arg. Est. (Ed.), Geografía de la República Argentina. GAEA, II (1), Buenos Aires, pp. 1–541.

Gulisano, C.A., Gutiérrez Pleimling, A.R., Digregorio, J.H., 1984. Esquema estratigráfico de la secuencia jurásica del oeste de la provincia de Neuquén. Actas IX Cong. Geol. Arg., vol. 1, pp. 221–235.

Hambling, A.P., Walker, R.G., 1979. Storm-dominated shallow marine deposits: the Fernie–Kootenay (Jurassic) transition, southern Rocky mountain. Can. J. Earth Sci. 16, 1673–1690.

Hampson, G.J., Storms, E.A., 2003. Geomorphological and sequence stratigraphic variability in wave-dominated. Shoreface-shelf parasequences. Sedimentology 50, 667–701.

Handford, C.R., 1986. Facies and bedding sequences in shelf-storm-deposited carbonates—Fayetteville Shale and Pikin Limestone (Mississippian) Arkansas. J. Sediment. Petrol. 56, 123–137.

Haq, B.U., Hardenbol, J., Vail, P.R., 1987. Chronology of fluctuating sea level since the Triassic. Science 235, 1156–1167.

Howard, J.D., Frey, R.W., 1984. Characteristic trace fossils in nearshore to offshore sequences, Upper Cretaceous of east-central Utah. Can. J. Earth Sci. 21, 200–219.

Insalaco, E., 1996. The use of late Jurassic coral growth bands as palaeoenvironmental indicators. Palaeontology 39, 413–431.

James, N.P., 1983. Reefs. In: Scholle, P.A., Debont, D.G., Moore, C.H. (Eds.), Carbonate Depositional Environments. Am. Ass. Petrol. Geol., Mem., vol. 33, pp. 345–440.

James, N.P., Choquette, P.W., 1984. Diagenesis 9. Limestones, the meteoric diagenetic environment. Geosci. Can. 11, 161–194.

Kamola, D., Van Wagoner, J.C., 1995. Stratigraphy and facies architecture of parasequences with examples from the Spring Member, Blackhawk Formation, Utah. In: Van Wagoner, J.C., Bertram, G.T. (Eds.), Sequence stratigraphy of foreland basin deposits: outcrops and subsurface examples from the Cretaceous of North America. Am. Ass. Petrol. Geol. Mem., vol. 64, pp. 27–64.

Ketcher, K., Allmon, W.D., 1993. Environment and mode of deposition of a Pliocene Coral Bed: coral thickets and storms in the fossil record. Palaios 8, 3–17.

Kidwell, S.M., 1991. The stratigraphy of shell concentration. In: Allison, P.A., Briggs, D.E.G. (Eds.), Taphonomy: Releasing the data locked in the Fossil record, Topics in Geobiology, vol. 9. Plenum Press, New York, pp. 211–290.

Kidwell, S.M., Fürsich, F.T., Aigner, T., 1986. Conceptual framework for the analysis and classification of shell concentrations. Palaios 1, 228–238.

Kidwell, S.M., Holland, S.M., 1991. Field description of coarse bioclastic fabrics. Palaios 6, 426–434.

Kreisa, R.R., 1981. Storm-generated sedimentary structures in subtidal marine facies with examples from the Middle and Upper Ordovician of Southwestern Virginia. J. Sediment. Petrol. 51, 832–848.

Leanza, H.A., 1981. The Jurassic–Cretaceous boundary beds in west-central Argentina and their ammonite zones. Neues Jahrb. Geol. Paläeontol., Abh. 161, 62–92.

Leckie, D.A., Walker, R.G., 1982. Storm and tide dominated shorelines in Cretaceous Moosebar–Lower gates interval-outcrop equivalents of deep basin gas traps in Western Canada. Am. Assoc. Petrol. Geol. Bull. 18, 138–157.

Legarreta, L., 1991. Evolution of a Callovian–Oxfordian carbonate margin in the Neuquén Basin of the west-central Argentina: facies,

architecture, depositional sequences and global sea-level changes. Sediment. Geol. 70, 209–240.

Legarreta, L., Gulisano, C.A., 1989. Análisis estratigráfico secuencial de la Cuenca Neuquina (Triásico Superior–Terciario Inferior), Argentina. Correl. Geol. (Universidad de Tucumán) 6, 221–243.

Legarreta, L., Uliana, M.A., 1996. The Jurassic succession in west central Argentina: Stratal patterns, sequences, and paleogeographic evolution. Palaeogeogr. Palaeoclimatol. Palaeoecol. 120, 303–330.

Leinfelder, R.R., 1992. A modern type Kimmeridgian reef (Ota Limestone, Portugal): implications for Jurassic reef models. Facies 26, 11–34.

Lo Forte, G., Palma, R.M., 2002. Facies, microfacies and diagenesis of Late Callovian–Early Oxfordian carbonates (La Manga Formation) in the west-central Argentinian High Andes. Carbon. Evap. 17 (1), 1–16.

MacEachern, J.A., Pemberton, S.G., 1992. Ichnology and event stratigraphy; the use of trace fossils in recognizing tempestites. In: Pemberton, S.G. (Ed.), Application of ichnology to petroleum exploration. SEPM Core Workshop, vol. 17, pp. 169–198.

Mitchum Jr., R.M, Uliana, M.A., 1985. Seismic stratigraphy of carbonate depositional sequences, Upper Jurassic–Lower Cretaceous. Neuquén Basin, Argentina. In: Berg, R.B., Woolverton, D.G. (Eds.), Seismic Stratigraphy: an integrated Approach to Hydrocarbon Exploration. Am. Assoc. Petrol. Geol. Memoir, vol. 39, pp. 255–274.

Morsch, S.M., 1990. Corales (Scleractinia) de la extremidad sur de la Sierra de la Vaca Muerta, Formación La Manga (Oxfordiano), provincia del Neuquén, Argentina. Ameghiniana 27 (1–2), 19–28.

Palma, R.M., Lazo, D., Piethé, G., 2005. Facies de tormenta y trazas fósiles en la rampa media de la Formación La Manga, Bardas Blancas, Mendoza. Actas XVI Cong. Geol. Argentino, La Plata, vol. 3, pp. 155–156.

Palma, R.M., Lo Forte, G., 1998. Evidencias diagenéticas en la sección inferior de la Formación La Manga, Caloviano), Alta Cordillera–Mendoza–Argentina. VI Reunión Argentina de Sedimentología, pp. 93–95. Abstr.

Palma, R.M., Lo Forte, G., Lanes, S., 1997. Diagenesis of the Lower Callovian Member of La Manga Formation, Aconcagua Basin, Mendoza, Argentina. 18th Regional European Meeting of Sedimentology, Heidelberg, Germany. Heidelbergensis (1), 260–263.

Palma, R.M., Lo Forte, G., Lanés, S., Junken, E., 2002. Superficie paleokarstica en las calizas oxfordianas de la Formación La Manga, Cuenca Neuquina, sur de Mendoza. IX Reunión Argentina de Sedimentología, Córdoba, vol. 1, p. 121. Abstr.

Palma, R.M., Lo Forte, G., Piethé, R.D., Crousse, L., González Pellegri, E., Bressan, G., 2004. Biohermas de esponjas y tipos de microbialitas en la Formación La Manga (Oxfordiano), Cuenca Neuquina, Mendoza. X Reunión Argentina de Sedimentología, vol. 1, p. 126.

Palma, R.M., Rodríguez, M., M, Lanes G., Lo Forte, G., Piethe, R.D., 2003. Las facies de esponjas y microbiolitas en la Formación La Manga (Oxfordiano), Cuenca Neuquina. Simposio Argentino sobre el Jurásico, La Plata, Argentina. p.12.

Peryt, T.M., 1983. Oncoids: comments to recent developments. In: Peryt, T.M. (Ed.), Coated Grains. Springer, Verlag, pp. 273–275.

Plint, A.G., Norris, B., 1991. Anatomy of a ramp margin sequence: facies successions, paleogeography and sediment dispersal patterns in the Muskiki and Marshybank Formations, Alberta foreland basin. Bull. Can. Pet. Geol. 39, 18–42.

Riding, R., 2000. Microbial carbonates: the geological record of calcified bacterial algal mats and biofilms. Sedimentology 47 (Supplement 1), 179–214.

Reineck, H.E., Singh, I.B., 1980. Depositional Sedimentary environments with reference to terrigenous clastics, 2nd ed. Springer–Verlag, Berlin, p. 551.

Riccardi, A.C., 1983. The Jurassic of Argentina and Chile. In: Moullade, M., Nairm, A.E.M. (Eds.), The Phanerozoic of the world II, The Mesozoic, B. Elsevier, Amsterdam, pp. 201–263.

Riccardi, A.C., 1984. Las asociaciones de amonitas del Jurásico y Cretácico de Argentina. IX. Cong. Geol. Argent., Actas, vol. 4, pp. 559–595.

Riccardi, A.C., 1992. Biostratigraphy of west-central Argentina. In: Westermann, G.E.G. (Ed.), The Jurassic of the Circum-Pacific. Cambridge University Press, pp. 139–141.

Schlager, W., 1989. Drowning unconformities on carbonate platforms. In: Crevello, P.D., Wilson, J.L., Sarg, J.F., Read, J.F. (Eds.), Controls on carbonate platform and basin development. Spec. Publ. Soc. Econ. Paleontol. Mineral., vol. 44, pp. 15–25.

Schlager, W., 1999. Type 3 sequence boundaries. In: Harris, P.M., Simo, J.A. (Eds.), Advances in Carbonate Sequence Stratigraphy: Application to Reservoirs, Outcrops and Models. Spec. Publ., vol. 63. SEPM, pp. 35–46.

Scoffin, T.P., 1987. An introduction to carbonate sediments and rocks. Blackie Publication Co, New York. 274 pp.

Shinn, E.A., 1983a. Tidal flat environments. In: Schole, P.A., Bebout, D.G., Moore, C. (Eds.), Carbonate Depositional Environments. Am. Assoc. Petrol. Geol., Mem., vol. 33, pp. 171–210.

Shinn, E.A., 1983b. Birdeyes, fenestrae, schrinkage pores and loferites: a re-valuation. J. Sediment. Petrol. 38, 215–223.

Stipanicic, P.N., 1951. Sobre la presencia del Oxfordense superior en el arroyo de La Manga, provincia de Mendoza. Rev. Asoc. Geol. Argent. 6 (4), 213–242.

Stipanicic, P.N., 1965. El Jurásico de la Vega de la Veranada (Neuquén), el Oxfordense y el diastrofismo divesano (Agassiz-Yailña) en Argentina. Asociación Geológica Argentina. Revista XX, vol. 4, pp. 403–478.

Stipanicic, P.N., 1969. El avance de los conocimientos del Jurásico argentino a partir del esquema de Groeber. Rev. Asoc. Geol. Argent. 24 (4), 367–388.

Stipanicic, P.N., 1996. Milestones in the study of the Jurassic of Argentina. In: Riccardi, A.C. (Ed.), Advances in Jurassic research. Geo. Research Forum, vol. 1–2, pp. 23–42.

Strasser, A., 1986. Ooids in Purbeck limestones (Lowermost Cretaceous) of the Swiss and French Jura. Sedimentology 33, 711–727.

Sweeting, M.N., 1973. Karst landforms. Columbia University Press, New York. 362 pp.

Swift, D.J.P., 1968. Coastal erosion and transgressive stratigraphy. J. Geol. 76, 444–456.

Tucker, M.E., Wright, V.P., 1990. Carbonate Sedimentology. Blackwell, Oxford. 482 pp.

Vail, P.R., 1987. Seismic stratigraphy interpretation using seismic stratigraphy, Part 1. Seismic stratigraphy interpretation procedure. In: Bally, A.W. (Ed.), Atlas of Seismic Stratigraphy. Am. Assoc. Pet. Geol., Stud. Geol., vol. 27, pp. 1–9.

Van Wagoner, J.C., Posamentier, H.W., Mitchum, R.M., Vail, P.R., Sarg, J.F., Louit, T.S., Hardenbol, J., 1988. An overview of the fundamentals of sequence stratigraphy and key definitions. In: Wilgus, Ch.K., Hastings, B.S., Kendall, CH. G. St. C. (Eds.), Sea-level changes: an integrated approach. Soc. Econ. Paleontol. Min. Spec. Publ., vol. 42, pp. 39–46.

Vergani, G.D., Tankard, A.J., Berlotti, H.J, Welsink, H.J., 1995. Tectonic evolution and palaeography of the Neuquén Basin, Argentina. In: Tankard, A.J., Suarez, R., Welsink, H.J. (Eds.), Petroleum Basins of South America. AAPG Memoir, vol. 62, pp. 383–402.

Walker, R.G., Plint, A.G., 1992. Wave and storm-dominated shallow marine systems. In: Walker, R.G., James, N.P. (Eds.), Facies Models: Response to sea level change. Geological Association of Canada, St. Johns, Newfoundland, pp. 219–238.

Westermann, G.E.G., 1967. Sucesión de ammonites del Jurásico Medio en Antofagasta, Atacama, Mendoza y Neuquén. Rev. Assoc. Geol. Argent. 22 (1), 65–73.

Westermann, G.E.G., Riccardi, A.C., 1984. Middle Jurassic Ammonite evolution in the Andean Province and emigration to Tethys. In: Friedman, G.M. (Ed.), Sedimentary and evolutionary cycles. Lec. Notes Earth Sci, vol. 1. Springer, Berlin, pp. 6–34.